Journal of Microencapsulation, 2013; 30(1): 81–92

ISSN 0265-2048 print/ISSN 1464-5246 online
DOI: 10.3109/02652048.2012.700957

informa
healthcare

Factorial design analysis and optimisation of alginate–Ca–chitosan microspheres

Liljana Makraduli, Maja Simonoska Crcarevska, Nikola Geskovski, Marija Glavas Dodov and Katerina Goracinova

Faculty of Pharmacy, Institute of Pharmaceutical Technology, University Ss Cyril and Methodius, Vodnjanska 17, 1000 Skopje, Macedonia

Abstract

The purpose of this study was to apply factorial design in order to determine the influence of the formulation factors and their interactions on several responses such as particle size, dissolution behaviour at pH 1.2 and pH 7.4 as well as production yield, during the development of budesonide loaded, chitosan coated Ca–alginate microparticles (MPs) intended for treatment of inflammatory diseases in the gastrointestinal tract. Produced drug-loaded MPs were spherical in shape, had smooth surfaces with low porosity and size range between 5 and 11 μm. Production yield for the formulations from the design varied from 19% to 50%. Optimisation was performed using central composite design setting the targets: particle size at 5.5 μm, maximised yield, suppressed dissolution at pH 1.2 and sustained release at pH 7.4. The optimised batches were identified with a combined desirability value of 0.967.

Keywords: central composite design, GIT inflammation targeting, spray drying, factorial design, chitosan–Ca–alginate, microparticles

Introduction

Budesonide (BDS)-loaded chitosan (CTS) coated Ca–alginate microparticles (MPs) for inflammation targeting were developed upon the targeting principle of enhanced epithelial cell permeability and increased activity and uptake function of the immune related cells at the site of inflammation. The abundant number of macrophages and dendritic cells during the inflammatory bowel disease (IBD), ulcerative colitis (UC) and Crohn's disease (CD) lead to increased interaction with physical systems, such as micro- and nanoparticles, increasing their concentration at the site of the disease and action. Improved localisation and prolonged residence time (locally in the inflamed tissue) might be achieved using MPs with an optimal particle size, probably between 4 and 15 μm (Tabata et al., 1996; Coppi et al., 2001; Lamprecht et al., 2001a, 2001b; Nakase et al., 2001; Coppi et al., 2002). Carrier systems in that size range are able to attach more efficiently to the mucus layer and accumulate in the inflamed region even without the need for macrophage uptake (Lamprecht et al., 2001a, 2001b). But also, further biological fate depends on the size and chemistry as well. It is reported that internalised particles between 2 and 5 μm will remain longer in Payer's patches, consequently showing very small systemic distribution compared to smaller nanosized particles.

Besides improved localisation, the drug delivery system should provide continuous release of the active substance at the site of action. But, BDS is a crystalline substance, practically insoluble in water with favourable pharmacokinetics (high topical/systemic availability) for local treatment of IBDs. Using spray-drying technique, incorporation of BDS in an amorphous state in the drug delivery system could be obtained (Tajber et al., 2009), thus improving its solubility and providing therapeutic concentration in a controlled manner at the site of action due to the properties of the system.

As most of the physico-chemical properties important for targeting and efficacy such as inertness, physico-chemical stability, swelling behaviour in the

Address for correspondence: Katerina Goracinova, Faculty of Pharmacy, Institute of Pharmaceutical Technology, University Ss Cyril and Methodius, Vodnjanska 17, 1000 Skopje, Macedonia. Tel: +38923126032, ext. 126. Fax: +38923123054. E-mail: kago@ff.ukim.edu.mk

(Received 17 Jan 2012; accepted 28 May 2012)
http://www.informahealthcare.com/mnc

bioenvironment of the upper gastrointestinal tract (GIT), zeta potential, dissolution rate as well as particle size might be controlled by the degree of alginate/CTS polyelectrolyte complexation and alginate/$CaCl_2$ ioniotropic gelation in these systems, the main objective of this article was to design a series of experiments to investigate the influence of several formulation factors (calcium chloride, CTS and BDS concentrations) on the above-mentioned variables (degree of swelling, particle size and dissolution rate) as well as production yield and their responses. MPs were prepared using one-step spray-drying procedure carried out through concomitant spraying of core (BDS containing alginate solution) and coating solutions (CTS/calcium chloride solution) through adopted two fluid nozzle. First of all, through ''one factor each time'' experiments, concentration range for CTS and alginate solutions operational for spray-drying processing as well as process conditions was established. Further, systematic approach in formulation development was performed, before an attempt of an optimisation to minimise the number of trials, study the influence of the factors and estimate the existence of significant interactions with certain precision as well as measure the change in response from one extreme of a factor to another, through structured 2^3 factorial design experiments, which was augmented to central composite design (CCD). CCD was used in the final stage of optimisation to obtain the equation composed of the main effects of the system, interactions of the factors and square effects that best describes the behaviour of the system within the limits of interest/(response surface).

Materials and methods

Materials

Low viscosity CTS, (molecular weight: 65–90 kDa, viscosity of 1% w/v aqueous solution in 2% v/v acetic acid: 130 mPa·s, deacetylation degree >80%) was purchased by Fluka, St. Gallen, Switzerland. Sodium alginate (Protanal LF 10/60, 65–75% of guluronic acid and 25–35% of manuronic acid content) was kindly donated by FMC BioPolymer, Haugesund, Norway. BDS was supplied from Crystal Pharma, Valladolid, Spain, and calcium chloride ($CaCl_2$) from Alkaloid, Skopje, Macedonia. All other applied materials were of analytical grade and used without any modifications.

Methods

Preparation of MPs

BDS was dispersed in sodium alginate solution in distilled water and $CaCl_2$ was added to 1% acetic acid CTS solution prior spray drying. Different formulations of CTS–Ca–alginate MPs were prepared using double nozzle and one-step spray-drying procedure (Buchi 290, Mini Spray Dryer, Buchi Labortechnik AG, Flawil, Swiss) (Simonoska Crcarevska et al., 2008; Glavas Dodov et al., 2009). Concentrations of CTS, $CaCl_2$ and BDS for the factorial design formulations were varied within the range of 1.0–2.5%; 0.5–2.0% and 1.0–3.0%, respectively. For the CCD formulations concentrations of $CaCl_2$, BDS and CTS were varied within the range of 0.17–2.33%, 0.56–3.44% and 0.67–2.83%, respectively.

Factor influence studies for process conditions for production of positively charged CTS coated Ca–alginate MPs by one-step-drying procedure, intended to be used as drug carriers for colon targeting were performed using different drug free batches (Goracinova, 2005). Based on these findings for the influence of feed composition, volume, flow rate, spray gas flow, inlet and outlet temperatures as well as aspirator capacity on the yield, particle size, zeta potential, moisture content, particle shape and morphology, process conditions for the design of formulation of drug-loaded MPs were carefully selected.

The process conditions employed for preparation of MPs were as follows: inlet temperature 170°C, outlet temperature 75°C, aspiration 100%, spray gas flow 700 L/h, feed flow 2 mL/min and feed solutions volume of 100 mL.

Production yields were determined as the weight percentage of the MPs obtained with respect to the initial amount of polymers and drug used for the microsphere preparation (De Jaeghere et al., 2001).

Characterisation of MPs

MPs shape and surface *morphology* were examined by a scanning electron microscope (SEM) (Jeol-SEM 6400, Tokyo, Japan). Samples were gold coated using a sputter coater.

Prepared MPs were characterised in terms of *particle size and particle size distribution* determined by laser diffractometer using Mastersizer 2000, Malvern Instruments Ltd, Worcestershire, UK, equipped with Hydro 2000S, Malvern Instruments Ltd, Worcestershire, UK, for wet dispersions ($n = 6$). Briefly, samples were dispersed in distilled water (20 mg/mL) and sonicated in ultrasonic bath for 5 min. Measurements were performed under stirring rate of 2520 rpm and 50% ultrasound, previously applied for 1 min. The obscuration was set between 10% and 12%. Particle size distribution was expressed in terms of SPAN factor as read from the measurement file. A high SPAN value indicates a wide size distribution (Dubey and Parikh, 2004).

Encapsulation efficacy i.e. BDS content in the MPs was determined and assayed by HPLC as it was previously described (Simonoska Crcarevska et al., 2008).

MPs were dispersed in phosphate buffer pH 7.4 (1 mg/mL), thermostated at 37 ± 0.5°C on horizontal shaker (Unitronic OR, Selecta, Barcelona, Spain) (100 rpm) for 24 h, to ensure complete dissolution of the particles. Samples were centrifuged (Tehtnika Centric 322B, Železniki, Slovenia) at 4000 rpm for 15 min. Centrifugates were withdrawn, filtered through 0.45 μm membrane filter (Ministar RC 25, Sartorius, Göttingen, Germany) and assayed by HPLC. Commercial BDS is an epimeric mixture of two isomers which have the same pharmacological

activity patterns. Having in mind previous, and appositely to pharmacopeia requirements (Council of Europe, 2010) it is from crucial importance to achieve adequate separation of both epimers, that is accomplished under the conditions described below.

Analyses were performed on Agilent 1100 Series HPLC system, equipped with 1100 Quaternary Pump and Agilent 1100 DAD detector. The column used was LiChroCART 150-4.6, Purospher STAR RP-18 endcapped (5 μm) (Merck KGaA, Darmstadt, Germany) at 242 nm UV detection. The mobile phase was acetonitrile/water (35 : 65). Chromatographic conditions for this method were: flow rate 1 mL/min, column temperature 25°C, injection volume 50 μL. Encapsulation efficiency was calculated as follows:

$$EE(\%) = \frac{\text{Actual drug loading}}{\text{Theoretical drug loading}} \times 100. \quad (1)$$

Zeta potential (ζ) of CTS–Ca–alginate MPs containing BDS was measured using Zetasizer Nano Series, Nano-ZS, Malvern Instruments Ltd, Worcestershire, UK. Measurements were performed after suspending the samples in acidic buffer pH 1.2 and phosphate buffer pH 7.4 (1 mg/mL) ($n = 6$).

Swelling properties of the CTS–Ca–alginate MPs were determined in acidic pH 1.2 and phosphate buffer pH 7.4, namely MPs dispersed in swelling solution (8 mg/mL) were continuously stirred on magnetic stirrer (300 rpm stirring rate) at room temperature. Measurements were performed, in predetermined time interval (1, 3 and 5 h), by laser diffractometry using Mastersizer 2000, Malvern Instruments Ltd, Worcestershire, UK, equipped with Hydro 2000S, Malvern Instruments Ltd, Worcestershire, UK, for wet dispersions ($n = 6$), under similar conditions as for particle size determination.

Swelling behaviour is presented as the volume increase ratio (VIR), in predetermined time interval, and it was calculated according to Equation (2):

$$\text{VIR ratio} = \frac{\text{A}d_{50}(\mu\text{m})}{\text{B}d_{50}(\mu\text{m})}, \quad (2)$$

where A is the particle diameter d_{50} (μm) of the swollen MPs incubated in different swelling solutions (pH 1.2 and 7.4) and B the particle diameter d_{50} (μm) of the MPs measured in water.

Differential scanning calorimetry (DSC) scans were recorded using a differential scanning calorimeter Mettler Toledo DSC-882 (Mettler, Greifensee, Switzerland). Samples were accurately weighed into 40 μL aluminium pans and heated from 25°C to 350°C at a heating rate of 10°C/min under a nitrogen flow rate of 50 mL/min.

Dissolution profiles of BDS from MPs were determined as follows. Quantity of MPs equivalent to 10 μg BDS was dispersed in 10 mL of dissolution medium and placed in closed glass tubes. The samples were kept at 37 ± 0.5°C with continuous shaking (100 rpm for 24 h) on horizontal shaker (Unitronik OR, Selecta, Barcelona, Spain). At appropriate intervals (1, 3, 5, 8 and 24 h), 1 mL samples were withdrawn, replaced by 1 mL of fresh buffer. The amount of BDS in the release medium was assayed by HPLC method previously described (Simonoska Crcarevska et al., 2008). The dissolution tests were performed under sink conditions and in triplicate ($n = 3$).

The dissolution pattern was assessed using DDSolver 1.0 (menu-driven add-in program for Microsoft Excel). It was evaluated to check the goodness of fit to the Korsmeyer–Peppas power law equation (Korsmeyer et al., 1983; Peppas, 1985) (Equations (3) and (4)) and fitting the data to the heuristic model proposed by Peppas and Sahlin (1989) (Equation (5)) for describing the phenomena controlling the release from swellable matrix, in which the contribution of the relaxation or erosion mechanism and of the diffusive mechanism can be quantified. The goodness of fit was evaluated using the r (correlation coefficient) values.

$$M_t/M_\infty = Kt^n. \quad (3)$$

This in logarithmic form is:

$$\log(M_t/M_\infty) = \log K + n \log t, \quad (4)$$

where M_t is the amount of drug dissolved in time t, M_∞ the amount of drug dissolved after infinite time (the drug content in the formulation), M_t/M_∞ the fractional release of the drug within time t, K the constant incorporating the structural and geometric characteristics of the dosage form, n the release (diffusion) exponent, which depends on the release mechanism and the shape of the matrix tested and t the release time. Exponent n for polymeric controlled delivery systems of spherical geometry has values of $n = 0.43$ for Fickian diffusion, $0.43 < n < 0.85$ for anomalous transport and $n > 0.85$ for Super case-II transport (Ritger and Peppas, 1987).

$$M_t/M_\infty = K_1 t^{1/2} + K_2 t, \quad (5)$$

where M_t is the amount of drug dissolved in time t, M_∞ the amount of drug dissolved after infinite time (the drug content in the formulation), M_t/M_∞ the fractional release of the drug in time t and K_1 and K_2 are the diffusion and erosion terms, respectively. According to this equation, if the diffusion to erosion ratio $K_1/K_2 = 1$, then the release mechanism involves diffusion and erosion equally. If $K_1/K_2 > 1$, then diffusion prevails, while erosion predominates when $K_1/K_2 < 1$ (Toti and Aminabhavi, 2004).

Experimental design

The purpose of the first experimental design step was to identify the components of the polyelectrolyte matrix, showing significant effect on the response parameters such as particle size, swelling and dissolution rate of BDS at different pH values. A 2^k factorial design with three replicates was designed, consisting of 24 runs (three factor interaction model), in order to investigate the main effects that influence the system and the interactions among factors (main effects of single factors: A, B, C; second-order (two-factor) interactions: AB, AC, BC and third-order (three-factor) interaction: ABC). The levels of the three independent variables (Table 1) were varied according to

Table 1. Coded units for 2^3 factorial design.

Factor	Level	
	Low	High
A	0.5	2.0
B	1.0	3.0
C	1.0	2.5

Notes: A, calcium chloride concentration (w/w, %); B, BDS concentration (w/w, %) and C, CTS concentration (w/w, %).

Table 2. Points for the investigated variables of the CCD augmented from 2^3 factorial design.*

Sequence number	Level of variables		
	A: $CaCl_2$	B: BDS	C: CTS
1	0.50	3.00	2.50
2	0.50	3.00	1.00
3	2.00	1.00	2.50
4	0.50	1.00	2.50
5	0.50	3.00	1.00
6	2.00	1.00	1.00
7	0.50	1.00	1.00
8	0.50	1.00	1.00
9	2.00	3.00	1.00
10	0.50	3.00	2.50
11	2.00	1.00	1.00
12	2.00	1.00	1.00
13	0.50	1.00	2.50
14	2.00	3.00	2.50
15	0.50	1.00	1.00
16	2.00	3.00	1.00
17	0.50	3.00	2.50
18	2.00	1.00	2.50
19	2.00	3.00	1.00
20	2.00	3.00	2.50
21	2.00	1.00	2.50
22	0.50	1.00	2.50
23	0.50	3.00	1.00
24	2.00	3.00	2.50
25	0.17	2.00	1.75
26	2.33	2.00	1.75
27	1.25	0.56	1.75
28	1.25	3.44	1.75
29	1.25	2.00	0.67
30	1.25	2.00	2.83
31	1.25	2.00	1.75
32	1.25	2.00	1.75
33	1.25	2.00	1.75

Notes: A, calcium chloride concentration (w/w, %); B, BDS concentration (w/w, %) and C, CTS concentration (w/w, %).
*Treatments 1–24 are the factorial points in the design; treatments 25–30 are the star points and 31–33 are the system-recommended centre points.

the design matrix shown in Table 2 (1–24). The experiments were carried out in a randomised order. The high *G* alginate *LF* 10/60 was used throughout the design and its concentration was kept constant (2%). The effect of the independent variables was investigated on the following responses: particle size, degree of swelling and dissolution rate at pH 1.2 and 7.4.

The addition of *centre points* to the design was the following step performed in order to check whether the linearity of the effects is a reasonable assumption or whether quadratic terms should be added to the model. Since the curvature was significant, further on, another model was used for modelling the curvature and unbiased factorial point prediction as well as to avoid aliasing of quadratic coefficients with one another.

As it is possible to obtain an equation composed of the main effects of the system, interactions of the factors and square effects using the CCD, this model was used in the final stage of optimisation to obtain the equations that best describes the behaviour of the system inside the limits of the region studied (response surface). This design was built from a 2^k factorial design with additionally included 2^k axial or ''star'' points and $n_0 \geq 2$ centre points. The axial points are located at a distance, α, from the design centre with a choice of $\alpha = \sqrt[4]{NF}$, where NF represents the number of factorial runs. The design points for CCD are presented in Table 2, treatments 1–24 are the factorial points in the design; treatments 25–30 are the star points and 31–33 are the system-recommended centre points (during the augmentation of the factorial design to a CCD additional set (block 2) of star and centre point runs were added to the factorial points). In this CCD design (central composite circumscribed design), the low and high values of each factor extended to create the star points were reasonable and applicable to one-step spray-drying procedure.

Six experimental responses were studied: Y_1, particle size; Y_2, drug release at pH 1.2 at the first hour; Y_3, drug release at pH 1.2 at the fifth hour; Y_4, drug release at pH 7.4 at the first hour; Y_5, drug release at pH 7.4 at the fifth hour and Y_6, the yield value. A classical second-degree model was postulated for each experimental response Y_i, as follows:

$$Y = b_0 + b_1\mathrm{A} + b_2\mathrm{B} + b_3\mathrm{C} + b_{11}\mathrm{A}^2 + b_{22}\mathrm{B}^2 + b_{33}\mathrm{C}^2 + b_{12}\mathrm{AB} + b_{23}\mathrm{BC} + b_{13}\mathrm{AC} + E_i, \quad (6)$$

where b_0 is the arithmetic mean response of the 33 runs, b_i the estimated coefficient while E_i is the experimental error for the factors, A, B and C.

The main effects (A, B and C) represent the average result of changing one factor at a time from its low to high value. The interaction terms (AB, BC and AC) show how the response changes when two factors are simultaneously changed. The polynomial terms (A^2, B^2 and C^2) are included to investigate nonlinearity. All experimental results were computed by statistical software, DOE v 8.0.6 (Stat-Ease, Inc., Minneapolis, MN).

In order to overcome the difficulties of multiple and opposing responses, optimisation of the responses was done using desirability method established by Myers and Montgomery (2002). The method makes use of an objective function, $D(X)$, called the desirability function. It reflects the desirable ranges for each response (d_i). Values of d_i are converted values for each response into an individual desirability function that varies over the range $0 \leq d_i \leq 1$. If the response is closer to the goal, then the d_i is close to 1 or 1 when it is at the goal, and if the response is outside

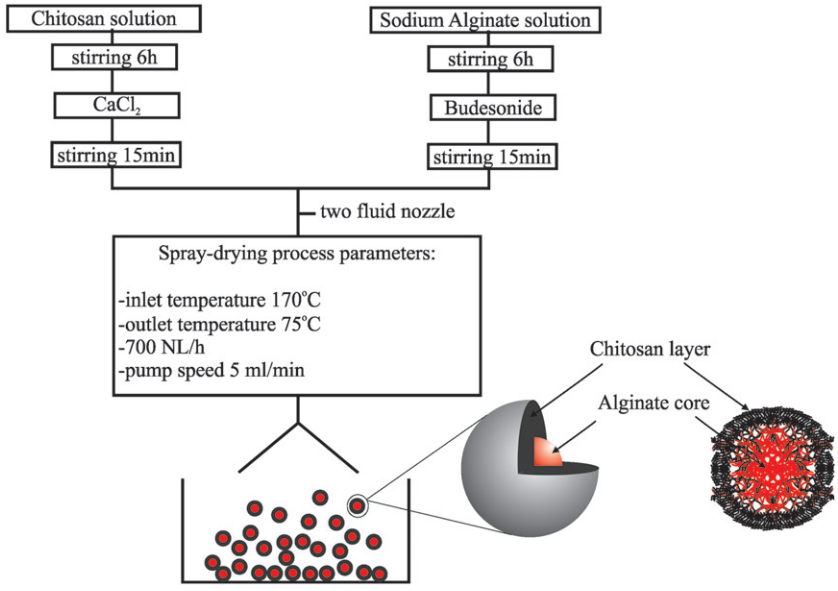

Figure 1. Schematic presentation of one-step spray-drying preparation procedure for BDS-loaded CTS–Ca–alginate MPs.

the accepted range then $d_i = 0$ (Prakobvaitayakit and Nimmannit, 2003). Subsequently, the simultaneous objective function will represent a geometric mean of all transformed responses (Equation (7)) (DOE v 8.0.6 Stat-Ease, Inc., Minneapolis, MN):

$$D = (d_1 x d_2 x d_3 \ldots x d_n)^{1/n} = \left(\prod_{i=1}^{n} d_i\right)^{1/n}, \quad (7)$$

where n is the number of responses in the measure. If any of the responses or factors falls outside their desirability range, the overall function becomes zero.

Cross-validation of the model and the per cent of relative error of the predicted and experimental values for each response for two independent check point batches was performed. Per cent bias for each response was calculated using the following equation:

$$\%\ \text{Bias} = \left[\frac{\text{PV} - \text{EV}}{\text{PV}}\right] \times 100, \quad (8)$$

where PV is the predicted value and EV the experimental value.

Results and discussion

Preparation of MPs

The method of preparation was simple and highly reproducible one-step spray-drying procedure (Goracinova, 2005; Goracinova et al., 2012) carried out through concomitant spraying of the core (alginate solution containing BDS) and coating solutions (CTS/calcium chloride solution) through adopted two fluid nozzle (Figure 1). Processes of ionotropic gelation/polyelectrolyte complexation are simultaneously performed during the short contact of the core and coating solution at the tip of the nozzle followed by drying in a spray-drying chamber. The process is very specific since both, CTS and calcium chloride, compete at the same time for negative alginate groups and the concentration of the polymers and employed process parameters have unique influence on the characteristic of the produced MPs as well as the process yield.

Characterisation of MPs and factorial design

Production yield was in a range from 19% to 50% and detailed values for the different formulations are presented in Table 3. The maximum yield of 50% is mainly due to the relatively low volumes of feed solutions sprayed for the preparation of each batch of MPs, the structure of the apparatus that is not equipped with a trap to recover the smaller and lighter particles exhausted by the aspirator and the loss of material mostly due to powder adhering to the cyclone walls (Glavas Dodov et al., 2009). Also, having in mind that production yield greatly depends on the concentration of the polymers as well as the concentration of the cross-linking agent, during the experimental design the yield was introduced as a response for further optimisation.

Surface morphology of the prepared CTS–Ca–alginate MPs is shown in Figure 2. Prepared MPs were with spherical morphology with presence of spherical discs with a collapsed centre. Surface appearance was smooth with low porosity. Insufficiency of ideal spherical morphology was most likely developed during the preparation procedure by spray-drying process.

Particle sizes (Table 3) ranging from d_{10} 1.131 ± 0.03 to $3.737 \pm 0.05\,\mu m$, d_{50} 5.653 ± 0.02 to $10.925 \pm 0.05\,\mu m$ and d_{90} 10.102 ± 0.04 to $39.786 \pm 0.09\,\mu m$ were obtained through 33 designed experiments in this study. Main factors and interactions influencing this parameter were calcium chloride concentration and calcium chloride/CTS concentration interaction as negative effects, as well as CTS and BDS concentration influence like positive effects (2^k factorial design). SPAN values were in range 1.5–4.

Table 3. Production yield and particle size of designed formulations.

Sequence number	Level of variables			Response	
	A: $CaCl_2$	B: BDS	C: CTS	Yield (%)	Particle size, d_{50} (μm)
1	0.50	3.00	2.50	21	10.9
2	0.50	3.00	1.00	34	6.9
3	2.00	1.00	2.50	24	7.5
4	0.50	1.00	2.50	19	9.9
5	0.50	3.00	1.00	32	8.5
6	2.00	1.00	1.00	20	6.5
7	0.50	1.00	1.00	28	6.4
8	0.50	1.00	1.00	26.7	6.9
9	2.00	3.00	1.00	28	6.9
10	0.50	3.00	2.50	22	10.9
11	2.00	1.00	1.00	20	6.5
12	2.00	1.00	1.00	23	6.5
13	0.50	1.00	2.50	21	8.6
14	2.00	3.00	2.50	19	7.8
15	0.50	1.00	1.00	27	7.4
16	2.00	3.00	1.00	20.4	6.3
17	0.50	3.00	2.50	22	10.
18	2.00	1.00	2.50	23.1	6.7
19	2.00	3.00	1.00	21	6.9
20	2.00	3.00	2.50	21.5	7.6
21	2.00	1.00	2.50	24	5.7
22	0.50	1.00	2.50	22	10
23	0.50	3.00	1.00	32.5	7.8
24	2.00	3.00	2.50	19.3	7.6
25	0.17	2.00	1.75	22	9.3
26	2.33	2.00	1.75	20	7.8
27	1.25	0.56	1.75	34	7.6
28	1.25	3.44	1.75	42	8.5
29	1.25	2.00	0.67	28	7.1
30	1.25	2.00	2.83	21	9
31	1.25	2.00	1.75	50	6.6
32	1.25	2.00	1.75	49	6.4
33	1.25	2.00	1.75	48.2	6.6

Notes: A, calcium chloride concentration (w/w, %); B, BDS concentration (w/w, %) and C, CTS concentration (w/w, %).

A high SPAN value indicates a wide size distribution (De Jaeghere et al., 2001). According to Gottlieb and Schwartzbach (2004), SPAN values lower than 2, for spray dried particles with d_{50} under 10 μm, indicate very narrow distribution. SPAN factor values for analysed MPs indicate narrow unimodal distribution. Particles within these size range and narrow particle size distribution resist the fast elimination from GIT due to the persistent diarrhoea experienced by the IBD patients and are eligible for improved accumulation and uptake into the inflamed tissue (Lamprecht et al., 2001a, 2001b; Simonoska Crcarevska et al., 2008; Glavas Dodov et al., 2009).

Encapsulation efficiency of BDS for all prepared formulations, determined by the HPLC method, was in the range between 94% and 102%. In fact, encapsulation efficiency was approaching the theoretical loading, due to the characteristics of the production process and because of its low variability it was not considered as a parameter for further optimisation.

DSC scans of sodium alginate, CTS, BDS and $CaCl_2$ are shown in Figure 3(A).

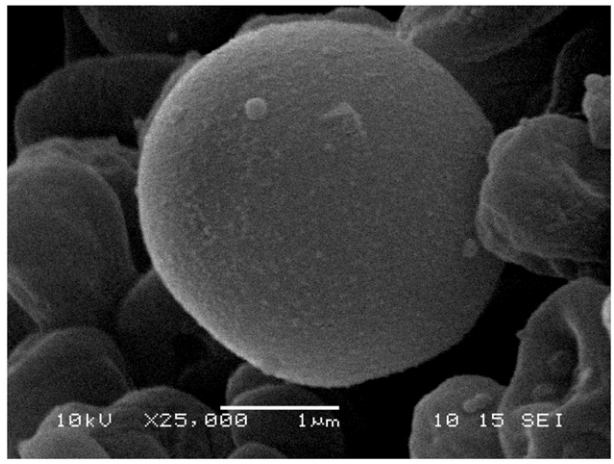

Figure 2. SEM micrographs of CTS–Ca–alginate MPs (sample 0.5$CaCl_2$/1BDS/1CTS).

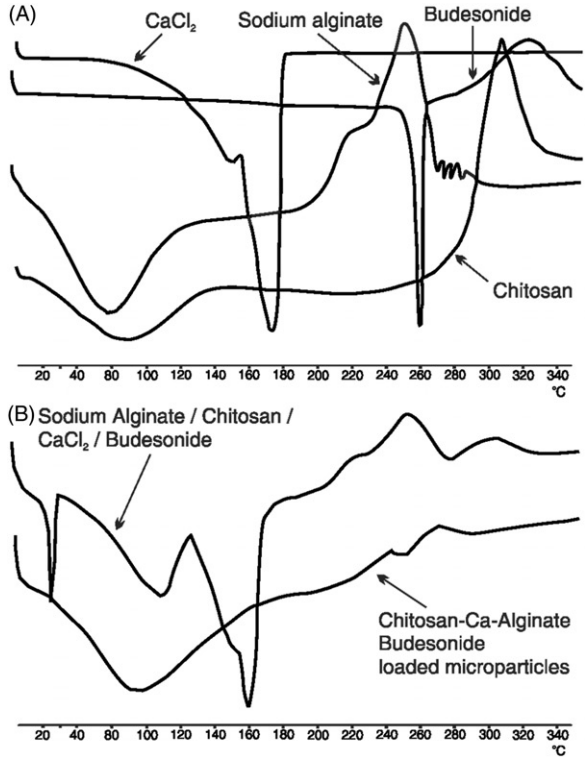

Figure 3. DSC scans of: (A) sodium alginate, CTS, calcium chloride and BDS and (B) CTS–Ca–alginate MPs loaded with BDS (0.5$CaCl_2$/3BDS/1CTS) and corresponding physical mixtures of sodium alginate/CTS/$CaCl_2$/BDS.

DSC scans of sodium alginate showed wide endothermic peak at 81.52°C that has been attributed to the evaporation of water, and appearance of an exothermic behaviour was detected starting around 200°C, with its maximum at 250.65°C, coinciding with the exothermic behaviour of the sodium alginate as referred to in several publications (González-Rodríguez et al., 2002) as the decomposition of the polymer. DSC scans of the CTS polymer exhibited an endothermic peak at 88.7°C that has been

attributed to the evaporation of absorbed water. The exothermic baseline deviation beginning around 250°C and gaining its maximum at 302.36°C indicates the onset of CTS degradation (González-Rodríguez et al., 2002; Borges et al., 2005). Sharp endotherm was observed for BDS at 257°C, corresponding to its melting transition point. Exotherm at 270°C refers to the onset of BDS degradation (Rodríguez et al., 1998). DSC scans of the $CaCl_2$ exhibited two endothermic peaks at 145.45°C and 169.52°C. Peaks in the DSC scans of the physical mixture (sodium alginate/CTS/$CaCl_2$/BDS) appeared to be a combination of each material but they are different from the DSC scans of the MPs (Figure 3B). Having in mind the characteristics and complexity of one-step spray-drying process and produced MPs, assembled through simultaneous polyelectrolyte complexation and ionotropic gelation due to the competition between positively charged Ca^{2+} and CTS for the negative charged alginate, we might assume that shifting of the exothermic peaks at 210°C and 250°C in the physical mixtures to 240°C and 270°C as well as disappearance of calcium chloride and CTS peaks in the MPs might be interpreted as interaction between the components of the system (Sankalia et al., 2007).

Disappearance of the drug melting peak in the DSC thermogram of drug-loaded formulation indicate the absence of the drug crystalline state in the delivery system. This evidence shows that drug loaded in the delivery system is in amorphous state of a solid molecular dispersion or a solid solution in the polymer matrix after encapsulation (Bandi et al., 2004; de Mello and Ricci-Júnior, 2011). So, entire absence of BDS endotherm in the MP thermograms propose that BDS is completely entrapped in the polymer matrix and also points to possibility of transformation of its crystal to amorphous structure, which probably occurs during preparation of MPs using the spray-drying technique (Wong et al., 2006; Simonoska Crcarevska et al., 2008).

Having in mind that positive *surface charge* is crucial for the interaction with negatively charged mucus and cell membranes, which might result with increased residence time in the GIT, our goal was to design and formulate a drug delivery system with positive surface charge. Moreover, due to the increased production of sialic acid and increased amount of negative sialic acid residues during the inflammation processes (Martinac et al., 2005) the affected surfaces might become even more negative. As the preparation process was designed in a manner for CTS to deposit as a coating layer around the alginate core, all formulations prepared during the experimental design showed positive zeta potential in the range of 30 ± 2–35 ± 3 mV and 8 ± 1.5–12 ± 2 mV at acidic buffer pH 1.2 and phosphate buffer pH 7.4, respectively. Taking into account that the measured zeta potential values were in a very narrow range, this parameter was not considered as a subject of the optimisation process.

Swelling behaviour of prepared MPs (from the factorial design) determined in buffers with pH 1.2 and pH 7.4 at the first, third and fifth hour is shown in Figure 4(A) and (B).

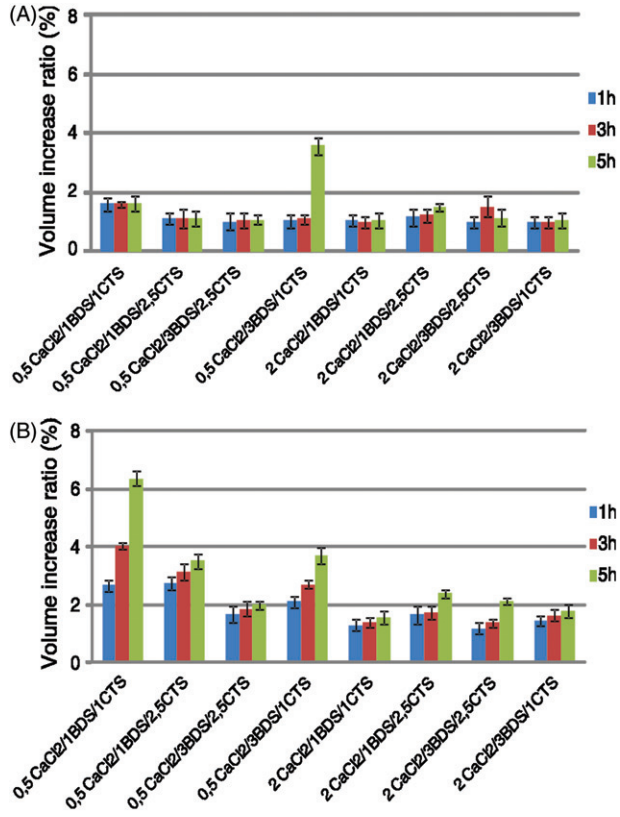

Figure 4. Swelling behaviour of BDS loaded CTS–Ca–alginate MPs in buffers at: (A) pH 1.2 and (B) pH 7.4 (mean ± SD, $n = 6$).

The VIR ratio in acidic pH at the first hour of swelling was in a range of 1.01 ± 0.02–1.62 ± 0.03, at the third hour 1.01 ± 0.04–2.97 ± 0.02 and at the fifth hour 1.01 ± 0.03–3.59 ± 0.02. The VIR ratio in pH 7.4 at the first hour of swelling was in a range of 1.19 ± 0.03–2.75 ± 0.04, at the third hour 1.38 ± 0.04–4.16 ± 0.05 and at the fifth hour 1.53 ± 0.03–6.85 ± 0.06. Actually, due to the matrix properties, in acidic pH only small degree of swelling was noticed, while at pH 7.4 excessive swelling and matrix destabilisation was observed. The swelling behaviour of MPs at pH 7.4 is most likely related to the exchange of Ca^{2+} ions from the polymer matrix with Na^{+} ions from the phosphate buffers (Bajpai and Sharma, 2004) and formation of calcium phosphate (Sutherland, 1991). Also, decreased binding of CTS with alginate due to the lower cationic nature of CTS at these conditions (*p*Ka of CTS is 6.2–7.0) (Ashford et al., 1993) influences the swelling. Factorial design pointed that factors influencing swelling at pH 1.2 were calcium chloride and CTS concentrations as well as their interactions (BDS/CTS, calcium chloride/BDS and calcium chloride/CTS interaction). Swelling properties at pH 7.4 were influenced by calcium chloride concentration (negative effect) and BDS concentration (positive effect) as well as mixed effects of calcium chloride/BDS concentration and BDS/CTS concentration.

Drug dissolution rate of the prepared MPs (the factorial design experiments) in buffers pH 1.2 and pH 7.4 simulating human GIT fluids is shown in Figure 5(A) and (B).

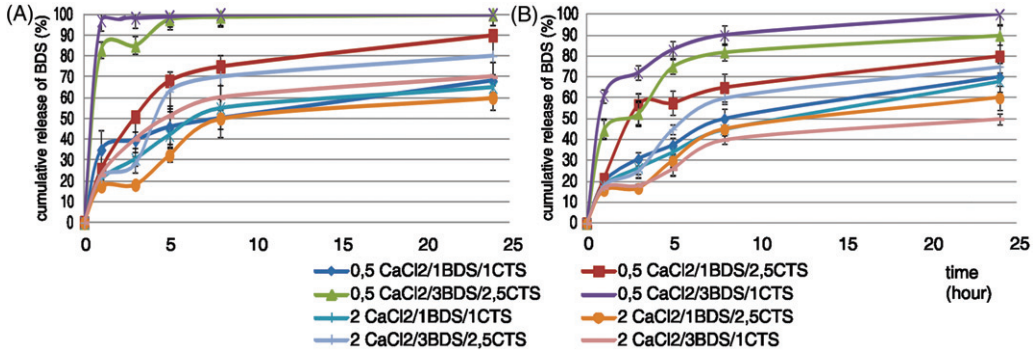

Figure 5. *In vitro* release profile of CTS–Ca–alginate MPs containing BDS in buffer at: (A) pH 1.2 at 37 ± 0.5°C (mean ± SD, $n = 3$) and (B) pH 7.4 at 37 ± 0.5°C (mean ± SD, $n = 3$).

Table 4. Comparison of dissolution kinetics models in pH 7.4.

	Korsmeyer–Peppas			Peppas and Sahlin			
	K	n	r	K_1	K_2	K_1/K_2	r
0.5$CaCl_2$/1BDS/1CTS	19.90	0.406	0.9931	20.31	−1.21	−16.78	0.9983
0.5$CaCl_2$/1BDS/2.5CTS	41.57	0.195	0.9004	33.88	−3.58	−9.46	0.9819
0.5$CaCl_2$/3BDS/2.5CTS	45.19	0.242	0.9597	43.67	−5.16	−8.46	0.9904
0.5$CaCl_2$/3BDS/1CTS	65.95	0.139	0.9907	53.67	−6.86	−7.82	0.9796
2 $CaCl_2$/1BDS/1CTS	17.51	0.428	0.9966	17.29	−0.69	−25.06	0.9985
2$CaCl_2$/1BDS/2.5CTS	13.74	0.473	0.951	14.76	−0.46	−32.08	0.9769
2$CaCl_2$/3BDS/2.5CTS	17.95	0.488	0.9316	21.96	−1.27	−17.29	0.9785
2$CaCl_2$/3BDS/1CTS	15.03	0.380	0.9514	14.86	−0.92	−16.15	0.9777
0.17$CaCl_2$/2BDS/1.75CTS	62.59	0.327	0.9012	79.62	−14.79	−5.38	0.9953
2.33$CaCl_2$/2BDS/1.75CTS	31.43	0.266	0.9791	29.67	−3.13	−9.47	0.9972
1.25$CaCl_2$/0.54BDS/1.75CTS	16.29	0.451	0.9501	10.22	−0.38	−26.9	0.991
1.25$CaCl_2$/3.44BDS/1.75CTS	32.37	0.248	0.9872	34.69	−3.34	−10.37	0.9878
1.25$CaCl_2$/2BDS/0.67CTS	28.58	0.295	0.976	28.63	−2.74	−10.46	0.9799
1.25$CaCl_2$/2BDS/2.83CTS	14.39	0.452	0.9899	14.14	−0.52	−27.22	0.9903
1.25$CaCl_2$/2BDS/1.75CTS	29.57	0.335	0.9662	21.2	−1.31	−16.21	0.999

In order to understand the release mechanism, the release data were fitted to empirical equations proposed by Korsmeyer–Peppas (Equation (4)) and Peppas and Sahlin (Equation (5)). Values of estimated parameters are given in Table 4. By comparing the values of the correlation coefficient (r) of different kinetic models, it can be clearly seen that release data showed best fitting to the heuristic model proposed by Peppas and Sahlin (1989) for quantifying the phenomena controlling the release from swellable matrix, in which the contribution of the relaxation or erosion mechanism and of the diffusive mechanism can be quantified. Since $K_1/K_2 < 1$, erosion dominantly controls drug release from matrix. These observations are in correlation with our previous studies concerning CTS–Ca–alginate MPs (Simonoska Crcarevska et al., 2008; Glavas Dodov et al., 2009).

Due to the importance of the particle size, production yield and dissolution rate for the efficacy of the designed system, these responses were further optimised using CCD. Particle size is crucial for improved localisation and prolonged residence time at the site of inflammation, while the dissolution rate is another element of major significance that should be considered for optimisation, having in mind that designed system had to posses abilities to suppress drug release in the upper part of GIT and at the same time to control drug release in the lower parts of GIT, finally resulting with improvement of the therapeutic efficacy.

Central composite design

Multiple regression and model building

During the factorial design studies independent variables (A: calcium chloride concentration; B: BDS concentration and C: CTS concentration) and their combined effects were identified as factors that highly influenced the yield, particle size and dissolution rate of BDS-loaded alginate–Ca–CTS MPs, and were used as independent variables for further studies. Due to the curvature that appeared after the inclusion of the central points to the design, the 2^k factorial model was augmented to CCD in order to obtain the equations supporting an unbiased description of the system and the region of interest. The developed models were tested for their significance using analysis of variance (ANOVA). Results were considered significant when the corresponding p-values were less than 0.05. During the CCD evaluation, dependent and independent variables

Table 5. ANOVA output statistics for the measured responses.

Response	Particle size (μm)	Dissolution 1 h, pH 1.2 (%)	Dissolution 1 h, pH 7.4 (%)	Dissolution 5 h, pH 1.2 (%)	Dissolution 5 h, pH 7.4 (%)	Yield (%)
SS	56.22	25 193.30	6769.44	15 795.76	10 278.06	1808.43
Degrees of freedom	9	9	9	9	9	9
Mean square	6.25	2799.26	752.16	2632.63	1142.01	200.94
F-value	20.81	91.11	40.86	46.97	49.50	49.26
Prob > *F*	<0.0001	<0.0001	<0.0001	<0.0001	<0.0001	<0.0001
SD	0.55	5.54	4.29	7.49	4.80	2.02
Mean	7.74	37.63	29.60	61.76	53.32	26.81
CV	7.08	14.73	14.50	12.12	9.01	7.53
PRESS	14.48	1790.19	1156.97	2454.85	1363.14	235.65
R^2	0.8949	0.9739	0.9436	0.9185	0.9529	0.9527
Adj-R^2	0.8519	0.9632	0.9205	0.8990	0.9337	0.9334
Pred-R^2	0.7696	0.9308	0.8387	0.8573	0.8736	0.8759
Adequate precision	15.551	27.119	19.103	18.887	23.792	26.027

were related through fitted polynomial equations and second-order regression models were developed based on the multiple regression analysis of the statistically significant variables for the responses: particle size, dissolution rate and yield value (ANOVA statistics for the fitted model is presented in Table 5). Predicted residual error sum of squares (PRESS) indicates how well the model fits the data. High values of correlation coefficient (R^2) for all dependent variables indicate a good fit. Adjusted R^2 (Adj-R^2) measures variation around the mean explained by the model, adjusted for the number of terms in model. The predicted R^2 (Pred-R^2) and the Adj-R^2 should be within 0.20 of each other. Otherwise there may be a problem with either the data or the model. Adj-R^2 and Pred-R^2 values were in reasonable agreement, signifying excellent model fit. Adequate precision value is greater than 4, indicating adequate model discrimination.

Polymer matrices prepared by polyelectrolyte complexation, additionally cross-linked by ionotropic gelation using inorganic calcium chloride, with pH-dependent swelling and dissolution, due to their complex nature often manifest various mixed effects with different magnitudes which are difficult to identify. The implemented model based on factorial design with three replicates augmented to CCD with additional axial and centre points, clearly distinguished among the factors of influence for the dissolution at different pH values and different time intervals. ANOVA pointed that drug dissolution (1 h) at pH 1.2 depends on the main factors and their interaction, as well as quadratic effect of the concentration of the ionotropic gelation agents. After 5 h at pH 1.2, according to the model, the influence of CTS appears to be insignificant, which is logical as CTS barrier might be dissolved within time in acidic environment. Factors influencing dissolution at pH 7.4 (1 h) are similar with those influencing the rate at pH 1.2 (1 h). At the fifth hour in the equation describing the release, negative quadratic effect of CTS appears as significant factor influencing release, which is in agreement with the polymer and MP properties, as well as expected barrier function of the CTS at higher pH values. The model equations describing the particle size (Equation (9)), yield (Equation (10)), the release after 1 h and 5 h, at pH 1.2 and pH 7.4 can be written as

$$\text{Particle size} = +6.07 - 0.82A + 0.36B + 0.76C - 0.51AC + 0.9A^2 + 0.65B^2 + 0.65C^2, \quad (9)$$

$$\text{Yield} = +50.87 - 1.82A + 1.09B - 2.15C - 1.21AB + 1.97AC - 1.13BC - 13.04A^2 - 4.84B^2 - 11.35C^2, \quad (10)$$

$$\text{Dissolution pH 1.2; 1h} = +17.00 - 19.85A + 14.41B - 6.39C - 12.89AB + 2.78AC + 19.59A^2, \quad (11)$$

$$\text{Dissolution pH 7.4; 1h} = +22.39 - 11.11A + 7.21B - 4.36C - 4.41AB + 2.52AC + 8.76A^2, \quad (12)$$

$$\text{Dissolution pH 1.2; 5h} = +62.27 - 19.23A + 12.51B - 4.96AB - 3.85AC, \quad (13)$$

$$\text{Dissolution pH 7.4; 5h} = +58.31 - 16.74A + 2.04B - 5.13C + 2.58AC + 7.92A^2 - 6.08B^2 - 8.74C^2. \quad (14)$$

The use of response surface plots allows visual observation of the significance of the regression equation by graphically depicting maxima and minima. Estimated surface plots illustrating the effect of calcium chloride × CTS (BDS = 2.00) for the responses: dissolution at pH 1.2 (1 h), dissolution at pH 7.4 (1 h), dissolution at pH 1.2 (5 h) and dissolution at pH 7.4 (5 h) are shown in Figure 6(A)–(D). It is obvious that the suppression of the dissolution rate at acidic pH depends on calcium chloride concentration and the level of ionic cross-linking. CTS concentration influence on the dissolution rate at pH 1.2 is not so pronounced as due to the polymer properties one cannot expect diffusion of CTS chains into the alginate droplet. As a consequence, CTS/alginate polyelectrolyte cross-linking will be

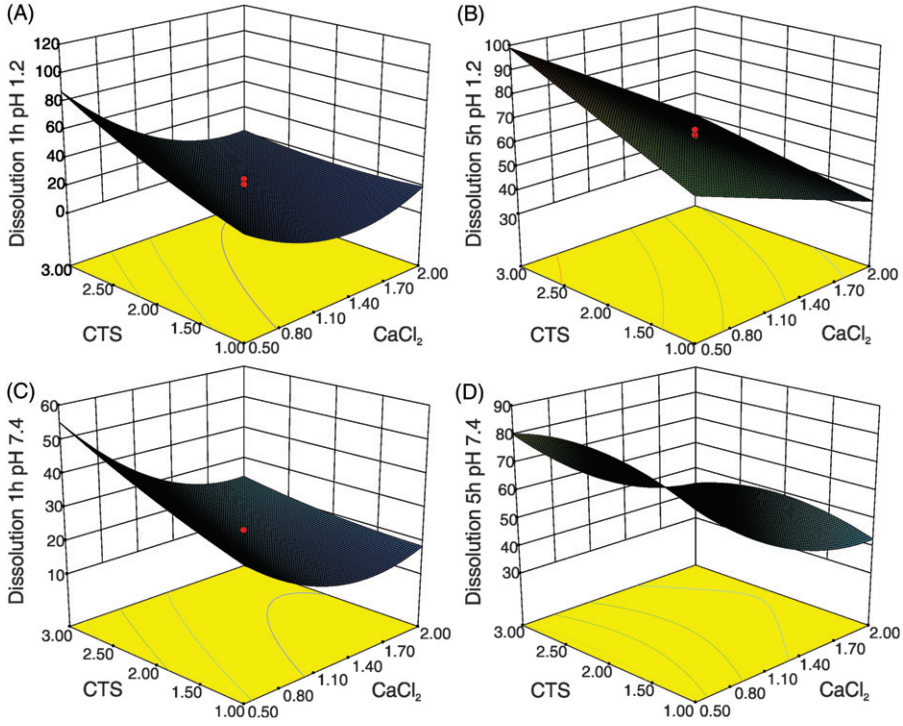

Figure 6. Surface plots illustrating the effect of calcium chloride × CTS (BDS = 2.00%) for the responses: (A) dissolution at pH 1.2 (1 h); (B) dissolution at pH 7.4 (1 h); (C) dissolution at pH 1.2 (5 h) and (D) dissolution at pH 7.4 (5 h).

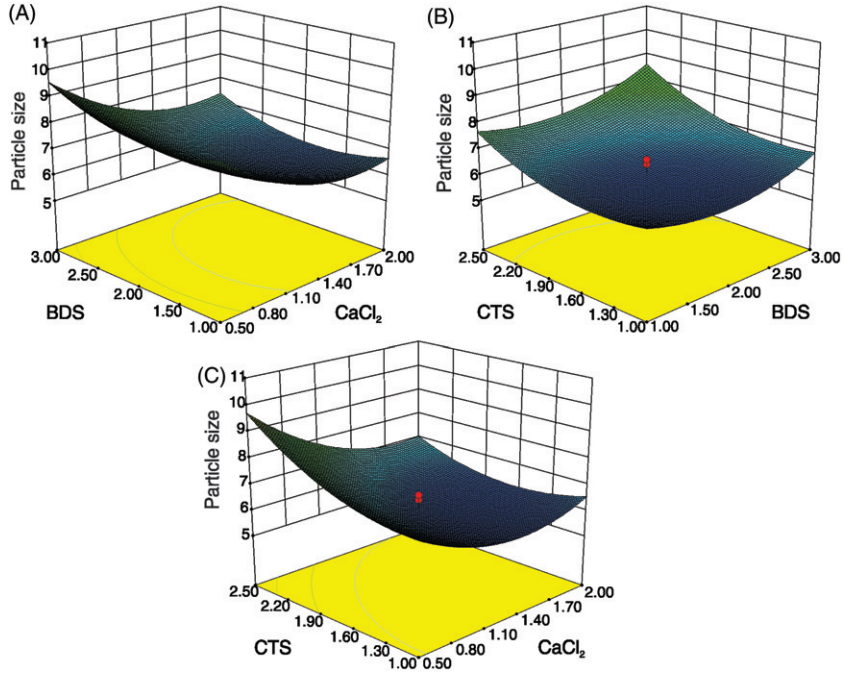

Figure 7. Surface plots illustrating the effect of formulation factors on particle size: (A) BDS × calcium chloride (CTS = 2.07%); (B) CTS × BDS (calcium chloride = 1.25%) and (C) CTS × calcium chloride (BDS = 2%).

located at the droplet surface compared to ionotropic gelation process spreading deeper into the alginate droplet. Moreover, CTS protective layer at the microsphere surface will be exposed to acidic medium which will immediately cause increased swelling and dissolution. The effect of the polyelectrolyte alginate/CTS cross-linking and CTS coating on the controlled release of the active substance is more pronounced at pH 7.4 due to its low solubility at basic pH. Total suppression of the release at pH 1.2 was not achieved for all combinations of factor levels (predicted interval for

Table 6. Optimised batches with predicted responses.

Number	$CaCl_2$ (%)	BDS (%)	CTS (%)	Particle size (μm)	pH 1.2 (%, 1 h)	pH 7.4 (%, 1 h)	pH 1.2 (%, 5 h)	pH 7.4 (%, 5 h)	Yield (%)
1	1.53	1.51	1.73	5.8643	8.8013	17.1317	50	51.0885	46.9571
2	1.52	1.50	1.73	5.8682	8.7414	17.1052	50	51.079	46.9722
3	1.52	1.50	1.74	5.8744	8.6858	17.0754	50	51.0465	46.9855

Figure 8. Individual and overall desirability for all measured responses.

Table 7. Composition of checkpoint formulations, the predicted and experimental values of response variables.

Number	$CaCl_2$ (%)	BDS (%)	CTS (%)	Particle size (μm) PV/EV	pH 1.2 (%, 1 h) PV/EV	pH 7.4 (%, 1 h) PV/EV	pH 1.2 (%, 5 h) PV/EV	pH 7.4 (%, 5 h) PV/EV	Yield (%) PV/EV
1	1.20	2.00	1.70	6.08/5.88	18.89/19.5	23.45/25	63.75/60.9	59.54/61.23	51.04
1-Bias (%)				3.24	−3.18	−6.60	4.48	−2.83	−2.05
2	1.52	2.00	1.50	5.76/5.67	14.5/13.26	20.55/22	56.63/58	53.85/55	47.89/50
1-Bias (%)				1.72	8.6	−7.04	2.40	−2.12	−4.30

Note: PV, predicted value; EV, experimental value.

minimal dissolution at pH 1.2 during the first hour was 7.0–12.0%; $\alpha = 0.05$; BDS not less than the midpoint of the interval). Sustained release at pH 7.4 over an extended period of time was achieved for different combinations of factor levels including the one that offered the lowest release rate at acidic pH (yield not less than 40%). Particle size as a factor important for the transit time, interaction at the level of mucus and gastrointestinal inflamed mucosa as well as a factor influencing the dissolution rate, should be kept at approximately 4–7 μm (d_{50}%) (Tabata et al., 1996; Lamprecht et al., 2001a). The design pointed that factors A, B, C, AC, A^2, B^2 and C^2 influenced significantly this response. Calcium chloride showed inverse effect on the size of the particles, but in the concentration range selected for the design highest salt concentrations resulted with larger particles, than the previous ones, which might be due to the specific conditions during the one-step spray-drying process, as 2% calcium chloride was close to the maximum concentration easily operated through two fluid nozzle. Higher concentrations produced agglomerates during the process of spray drying. Surface plots illustrating the effect of calcium chloride, CTS and BDS concentration on particle size are shown in Figure 7. Combinations of factor levels over the space of desired performance (lower release rate at pH 1.2; sustained release at pH 7.4; yield not less than 40%) resulted with particle size of 5–7 μm, size in a range to support the accumulation at the site of inflammation.

In the optimisation procedure target of 5.5 μm was set for particle size, drug release at pH 1.2 have to be minimised, yield maximised and dissolution at pH 1.2 and 7.4 (5 h) was set to be not more than 50%. Using the desirability function, all the measured responses were combined to get overall response, that is, the overall desirability. The overall desirability response was calculated from the individual desirability of each of the responses using DOE v8.0.5 (Stat-Ease, Inc., Minneapolis, MN). The optimised batches were identified with a combined desirability value of 0.967 for both solutions.

Table 6 enlists the optimised values for the independent variables. Individual and overall desirability for all measured responses is shown in Figure 8.

Confirmation report from the cross-validation of the model and the per cent of relative error of the predicted and experimental values are presented in Table 7.

Conclusion

Optimised formulations provide significant suppression of the release of the active substance at acidic pH, as well as slow and continuous BDS release at higher pH values. Although the system is based on the targeting principle of increased residence time due to the mucoadhesivity, positive zeta potential and increased interaction with highly permeable diseased tissue as well as higher accumulation in the inflamed tissue due to the physical interaction of the particles of particular size with the elements of the immuneregulatory system, additional pH-dependent coating will improve its targeting properties (targeting the release at the site of inflammation) especially in UC. As far as the other type of IBD is concerned, whether the system should be additionally coated will depend upon the localisation of the inflammation in CD.

Acknowledgements

The authors acknowledge the support of NATO SfP: 978023.

Declaration of interest

The authors report no conflicts of interest. The authors alone are responsible for the content and writing of this article.

References

Ashford M, Fell JT, Attwood D, Sharma H, Woodhead PJ. An in vivo investigation into the suitability of pH dependent polymers for colonic targeting. Int J Pharm, 1993;95(1–3):193–9.

Bajpai SK, Sharma S. Investigation of swelling/degradation behaviour of alginate beads crosslinked with Ca^{2+} and Ba^{2+} ions. React Funct Polym, 2004;59(2):129–40.

Bandi N, Wei W, Roberts CB, Kotra LP, Kompella UB. Preparation of budesonide– and indomethacin–hydroxypropyl-β-cyclodextrin (HPBCD) complexes using a single-step, organic-solvent-free supercritical fluid process. Eur J Pharm Sci, 2004;23(2):159–68.

Borges O, Borchard G, Verhoef JC, De Sousa A, Junginger HE. Preparation of coated nanoparticles for a new mucosal vaccine delivery system. Int J Pharm, 2005;299(1–2):155–66.

Coppi G, Iannuccelli V, Bernabei MT, Cameroni R. Alginate microparticles for enzyme peroral administration. Int J Pharm, 2002;242(1–2):263–6.

Coppi G, Iannuccelli V, Leo E, Bernabei MT, Cameroni R. Chitosan-alginate microparticles as a protein carrier. Drug Dev Ind Pharm, 2001;27(5):393–400.

Council of Europe. 2010. European pharmacopoeia. 7th edn. Strasbourg, France: Council of Europe.

De Jaeghere F, Allemann E, Cerny R, Galli B, Steulet AF, Muller I, Schutz H, Doelker E, Gurny R. pH-Dependent dissolving nano- and microparticles for improved peroral delivery of a highly lipophilic compound in dogs. AAPS PharmSci, 2001;3(1):E8.

de Mello VA, Ricci-Júnior E. Encapsulation of naproxen in nanostructured system: Structural characterization and in vitro release studies. Quim Nova, 2011;34:933–9.

Dubey RR, Parikh RH. Studies of PLGA microspheres. Pharm Technol Eur, 2004;16(5):23–34.

Glavas Dodov M, Calis S, Crcarevska MS, Geskovski N, Petrovska V, Goracinova K. Wheat germ agglutinin-conjugated chitosan-Ca-alginate microparticles for local colon delivery of 5-FU: Development and in vitro characterization. Int J Pharm, 2009;381(2):166–75.

González-Rodríguez ML, Holgado MA, Sánchez-Lafuente C, Rabasco AM, Fini A. Alginate/chitosan particulate systems for sodium diclofenac release. Int J Pharm, 2002;232(1–2):225–34.

Goracinova K. Formulation and preparation of spray-dried alginate–Ca microparticles. Patent no. MP/MK/05/01/FF/BE/01/IP, 2005.

Goracinova K, Glavas-Dodov M, Simonoska-Crcarevska M, Geskovski N. 2012. Drug targeting in IBD treatment – Existing and new approaches. In: Karoui S, ed. Inflammatory bowel disease – Advances in pathogenesis and management. In Tech Europe, Rijeka, Croatia, pp. 301-32, ISBN: 978-953-307-891-5.

Gottlieb N, Schwartzbach C. 2004. Development of an internal mixing two-fluid nozzle by systematic variation of internal parts. 19th Annual Meeting of ILASS (Europe) Conference Proceedings, Nottingham, UK, p. 97.

Korsmeyer RW, Gurny R, Doelker E. Mechanisms of solute release from porous hydrophilic polymers. Int J Pharm, 1983;15(1):25–35.

Lamprecht A, Schäfer U, Lehr CM. Size-dependent bioadhesion of micro- and nanoparticulate carriers to the inflamed colonic mucosa. Pharm Res, 2001a;18(6):788–93.

Lamprecht A, Ubrich N, Yamamoto H, Schäfer U, Takeuchi H, Maincent P, Kawashima Y, Lehr CM. Biodegradable nanoparticles for targeted drug delivery in treatment of inflammatory bowel disease. J Pharmacol Exp Ther, 2001b;299(2):775–81.

Martinac A, Filipovic-Grcic J, Perissutti B, Voinovich D, Pavelic Z. Spray-dried chitosan/ethylcellulose microspheres for nasal drug delivery: Swelling study and evaluation of in vitro drug release properties. J Microencapsul, 2005;22(5):549–61.

Myers HR, Montgomery CD. 2002. Response surface methodology: Process and product optimization using designed experiments. New York: Wiley & Sons.

Nakase H, Okazaki K, Tabata Y, Uose S, Ohana M, Uchida K, Nishi T, Debreceni AS, Itoh T, Kawanami C, et al. An oral drug delivery system targeting immune-regulating cells ameliorates mucosal injury in trinitrobenzene sulfonic acid-induced colitis. J Pharmacol Exp Ther, 2001;297(3):1122–8.

Peppas NA. Analysis of Fickian and non-Fickian drug release from polymers. Pharm Acta Helv, 1985;60(4):110–11.

Peppas NA, Sahlin JJ. A simple equation for the description of solute release. III. Coupling of diffusion and relaxation. Int J Pharm, 1989;57(2):169–72.

Prakobvaitayakit M, Nimmannit U. Optimization of polylactic-co-glycolic acid nanoparticles containing itraconazole using 2^3 factorial design. AAPS PharmSciTech, 2003;4(4):565–73.

Ritger PL, Peppas NA. A simple equation for desciption of solute release I. Fickian and non-Fickian release from non-swellable devices in the form of slabs, spheres, cylinders or discs. J Control Release, 1987;5(1):23–36.

Rodríguez M, Vila-Jato JL, Torres D. Design of a new multiparticulate system for potential site-specific and controlled drug delivery to the colonic region. J Control Release, 1998;55(1):67–77.

Sankalia MG, Mashru RC, Sankalia JM, Sutariya VB. Reversed chitosan–alginate polyelectrolyte complex for stability improvement of alpha-amylase: Optimization and physicochemical characterization. Eur J Pharm Biopharm, 2007;65(2):215–32.

Simonoska Crcarevska M, Glavas Dodov M, Goracinova K. Chitosan coated Ca–alginate microparticles loaded with budesonide for delivery to the inflamed colonic mucosa. Eur J Pharm Biopharm, 2008;68(3):565–78.

Sutherland IW, 1991. Alginates. In: Byrom D, ed. Biomaterials, novel materials from biological sources. New York: Stockton, pp. 309–31.

Tabata Y, Inoue Y, Ikada Y. Size effect on systemic and mucosal immune responses induced by oral administration of biodegradable microspheres. Vaccine, 1996;14(17–18):1677–85.

Tajber L, Corrigan DO, Corrigan OI, Healy AM. Spray drying of budesonide, formoterol fumarate and their composites—I. Physicochemical characterisation. Int J Pharm, 2009;367(1–2):79–85.

Toti US, Aminabhavi TM. Modified guar gum matrix tablet for controlled release of diltiazem hydrochloride. J Control Release, 2004;95(3):567–77.

Wong SM, Kellaway IW, Murdan S. Enhancement of the dissolution rate and oral absorption of a poorly water soluble drug by formation of surfactant-containing microparticles. Int J Pharm, 2006;317(1):61–8.